Netsu Sokutei **45** (2), 63-69 (2018)

Article

Thermodynamics and Kinetics of Aggregation of Myoglobin with 1,4-Dioxane

Tomokadu Marutani, Takashi Inomata, and Tadashi Kamiyama

Department of Science, School of Science and Engineering, Kindai University

(Received Dec. 7, 2017; Accepted Jan. 2, 2018)

The thermodynamic properties and state diagram of the thermally induced aggregation of myoglobin with 1,4-dioxane were determined by DSC, circular dichroism (CD), dynamic light scattering (DLS), scanning electron microscopy (SEM), and density measurements. At a mole fraction (x) of 1,4-dioxane of around 0.10, myoglobin exhibited α-helical aggregation at 25 °C, which transformed to spherical aggregation without thermal denaturation upon heating. The enthalpy change for the spherical aggregation was −565 kJ mol^{-1} at x = 0.10, which was numerically greater than that for thermal denaturation of the native state, 428 kJ mol^{-1}, indicating that the aggregate conformation involved many intermolecular interactions. At x = 0.125 − 0.25, the α-helix partially transformed to a β-sheet at 25 °C, which formed an amorphous aggregate upon heating. The thermal transition depends on the incubation time of the pre-transition state due to conformational changes in this state. The positive change in the partial specific volume of the aggregate indicates a large cavity volume and reduced hydration. On the other hand, the activation volume for the aggregation is negative, $(-4.5 \pm 1.3) \times 10^2$ cm^3 mol^{-1}, suggesting that the activated state has a structure with fewer cavities and/or is highly hydrated compared to the pre-transition state, probably due to partial unfolding.

Keywords: Aggregation, myoglobin, dioxane, DSC, state diagram, activation volume

1. Introduction

Protein conformations can be divided into various forms: the folded native state; the unfolded denatured state with loss of tertiary and secondary structure, which is present in the native state; an intermediate state such as a molten globule state; an aggregated state such as amorphous aggregation; and ordered aggregation such as fibrous aggregation. The folded native state has low stability due to a balance between enthalpic factors such as hydrophobic interactions, hydrogen bonding, and electrostatic interactions, and entropic factors derived from the protein conformation and solvation. Hence, the folded native state is easily transformed into other states by external perturbation resulting from temperature, pressure, and co-solvent.[1-3] Protein aggregation causes less desirable characteristics such as reduced or no biological activity, which occasionally leads to amyloid diseases.[4,5] Ordered aggregates have been observed in many proteins and are likely to be one of their basic structural forms.[6-8] Elucidating the aggregation mechanism is important for preventing protein diseases and for preserving protein solutions by understanding the misfolding process. The structures of aggregates have been revealed by nuclear magnetic resonance (NMR), X-ray structural analysis, and circular dichroism (CD).[9-11] However, there are limited thermodynamic data on the aggregation process.[12,13] One of the reasons for this is the difficulty in quantitatively interpreting changes in spectroscopic intensity, because aggregation inevitably leads to a decrease in protein solubility. Conversely, thermal analysis effectively compensates for data unavailable by spectroscopy, because thermal methods macroscopically observe whole reactions, including aggregated precipitation.

To clarify the aggregation mechanism, appropriate conditions for aggregating the protein must be selected to easily observe the aggregation process. Generally, one of the conditions for inducing aggregation is that the protein should be near its isoelectric point, which decreases the electrostatic repulsion between proteins. However, in many cases, aggregation produces an amorphous precipitate rather than an ordered form. Ultrasonication is an effective trigger for inducing aggregation,[14] but it is not easy to obtain thermal information on the aggregation process, because the ultrasonic waves create too large a thermal background. Recently, we found that cytochrome *c* formed an ordered fibrous aggregate upon heating in an appropriate mole fraction of dioxane in water, and we determined the state diagram and thermodynamics for the denaturation and aggregation of cytochrome *c*.[15] The addition of dioxane is a very simple and moderate perturbation compared to ultrasonic perturbation, so it allows precise thermal measurement. Protein aggregation often occurs continuously following denaturation at high concentrations for DSC measurements, because hydrophobic groups exposed by unfolding contribute to intermolecular association, resulting in thermal peak overlap.[16,17] Therefore, in most cases, it would be difficult to quantitatively estimate the thermodynamic properties of each transition. However, addition of dioxane separates the transition peaks for denaturation and aggregation, making it possible to determine the change in enthalpy and midpoint temperature for each transition.

In this study, we have determined the thermodynamics of the thermal denaturation and aggregation of myoglobin in the presence of 1,4-dioxane by differential scanning calorimetry (DSC). The structure in solution and precipitated myoglobin were measured by CD, dynamic light scattering (DLS), and scanning electron microscopy (SEM). The influences of the mole fraction of dioxane, incubation time, and pressure on the aggregation were thermodynamically and kinetically analyzed. Myoglobin is a good model protein, since it is typically globular and monomeric, and there are many reports on its non-native states including its ordered aggregation.[18,19] Myoglobin is a heme protein like cytochrome *c*, which we have previously studied with respect to its aggregation.[15] Myoglobin has a porphyrin ring with a non-covalent bond, while cytochrome *c* binds with a covalent thioether bond. The compressibility of myoglobin, which reflects the flexibility of the structure, is 8.98

$\times 10^{-5}$ MPa^{-1}, which is significantly larger than the value of 0.066 $\times 10^{-5}$ MPa^{-1} for cytochrome *c*.[20] This thermodynamic and conformational information shows that myoglobin has a more flexible conformation than cytochrome *c*, indicating that myoglobin is an appropriate model protein for discussing the influence of flexibility on aggregation.

2. Material and methods

2.1 Materials

Horse heart myoglobin was purchased from Sigma-Aldrich. Myoglobin was dialyzed with Milli-Q water. The concentration of myoglobin in a stock protein solution was determined by absorbance measurements. The 1,4-dioxane (Kanto Chemical, prime pure grade) was dehydrated using freshly activated grade 4A molecular sieves under a reduced pressure of 0.3 kPa at 327 K. The sample solutions were prepared by mixing given weights of the stock protein solution, dioxane, and water. The final concentrations of myoglobin and the mole fraction of dioxane were determined using dilution factors obtained from the gravimetric and density data for the solvents and solutions. In calculating the mole fraction of 1,4-dioxane (x) for ternary solutions, water (1) + 1,4-dioxane (2) + myoglobin (3), these could be regarded as two-component systems of water and 1,4-dioxane, because the amount of myoglobin was negligible compared with the amounts of 1,4-dioxane and water.

2.2 Methods

2.2.1 DSC

The thermal transition of myoglobin was monitored using a high-sensitivity differential scanning calorimeter (Micro DSC VII evo, SETARAM) at a scanning rate of 1 K min^{-1}. The protein concentration of the solutions was approximately 0.50 % w/v. The volume of solution in the DSC cell was approximately 0.7 ml. All sample solutions and reference solvents were degassed at least 5 min before DSC measurements. After the measurements, the DSC cell was filled with 6 M urea for 30 min and washed with water to remove any protein contamination.

2.2.2 Spectroscopy

CD of myoglobin was measured using a J-820 CD spectrophotometer (JASCO) with a PTC-348WI temperature control system. The cell length was 1.0 mm and the concentration of myoglobin was approximately 0.05 % w/v. The scanning rate was 1 K min^{-1}. DLS was performed using a Zetasizer Nano ZSP (Malvern) instrument with a quartz cell (ZEN2112). The protein concentration was approximately 0.5 % w/v. SEM images of aggregated myoglobin were obtained using an S-4800 scanning electron microscope (HITACHI) with an accelerating voltage of 5.0 kV. The aggregates obtained after DSC measurements were thoroughly dried under vacuum at room temperature and coated with osmium.

2.2.3 Density

Density measurements were performed using a high precision densimeter (DMA 512, Anton Paar, Austria), which was designed to measure the density under pressures of up to 40 MPa. The period of harmonic oscillation of the cell, reflecting the density, was monitored with a universal counter (SC-7205, Iwatsu, Japan). The resolution of the period corresponds to a density of about 1 $\times 10^{-6}$ g cm^{-3}. Pressure was applied by pumping water with a hand pump (FHP-5, RIKEN SEIKI) and a cylinder (S04-70, RIKEN SEIKI). The pressure was monitored using a digital pressure gauge (DPS-700S, RIKEN SEIKI) with an accuracy of 0.001 MPa. The temperature was controlled to within 0.001 °C with a circulating water bath (Thermocirculator, TC-100, Tokyo Riko) and was monitored with a digital thermometer (4600, YSI). All data were fed to a personal computer at 10 s intervals via a RS-232C interface. The apparent partial specific volume of the protein (v^*) at a given pressure was calculated using the following equation

$$v^* = (1/m^*)\,[1-(d_s^*-m^*)/d_0^*] \quad (1)$$

where d_0^* and d_s^* are the densities of the solvent and protein solution at the given pressure, respectively, and m^* is the protein concentration in g cm^{-3}, which was calibrated to the pressure using the relation $m^* = m\,(d_s^*/d_s)$, where m and d_s are the protein concentration and the solution density, respectively, at atmospheric pressure. The protein concentration is approximately 0.5 % w/v.

3. Results and discussion

3.1 CD of myoglobin with dioxane at room temperature

The thermodynamic change in conformational transitions of proteins reflects the difference in protein structure before and after the transition. To reveal the thermodynamics of thermally induced aggregation, it is necessary to determine the structure not only before but also after the transition. CD is an effective and convenient approach for observing changes in protein structure, especially secondary structures, in solution. **Fig.1(a)** shows CD spectra of myoglobin in aqueous 1,4-dioxane solution at various mole fractions (x) at 25 °C just after sample preparation. The molar ellipticity at 222 nm reflects the amount of secondary structure of the protein,[21] which is plotted against the mole fraction of dioxane in **Fig.1(b)**. The shape and intensity of the spectrum of myoglobin in water at x = 0 indicated that myoglobin has a rich α-helical structure in the native state. For x < 0.05, the shape and intensity are similar to in the native state. However, at x = 0.05 – 0.10, the intensity significantly decreased, while the shape remained similar to that of the native state. A fine red precipitate was observed in the solution at room

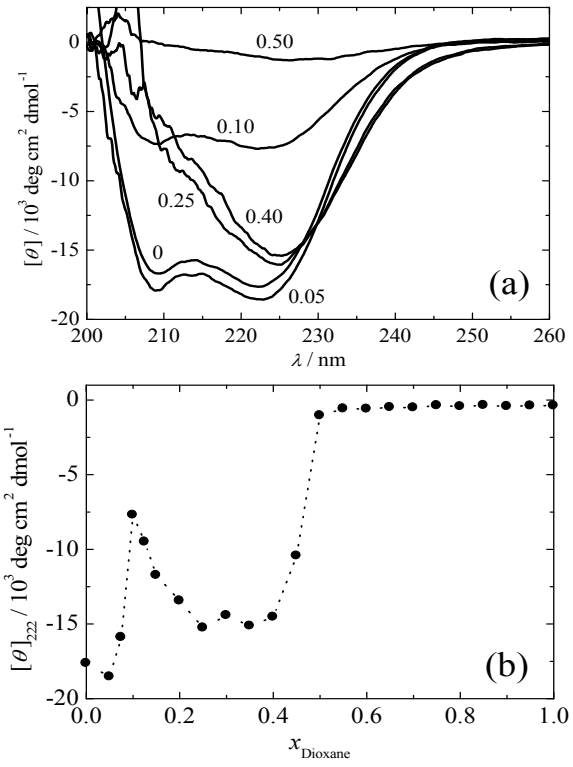

Fig.1 (a) CD spectra of myoglobin in (1−x) water + x 1,4-dioxane. The number beside the line is the mole fraction of dioxane, x. (b) Plot of $[\theta]_{222}$ of myoglobin against x. The molar ellipticities were calculated from the protein concentration at sample preparation, ≈ 0.05 %.

temperature. The size of the particles in the solution was determined as about 320 nm by DLS, indicating that myoglobin aggregated, because the size of the native state was about 3.5 nm as determined by DLS in water, as shown in **Fig.2**. These results indicate that the significant decrease in the intensity of the molar ellipticity is due to a decrease in the concentration of myoglobin resulting from aggregation.

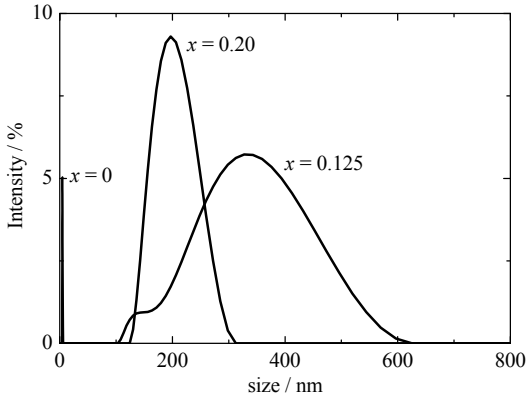

Fig.2 DLS results of myoglobin in (1−x) water + x 1,4-dioxane. The number beside the line is the mole fraction of dioxane, x.

At x = 0.125 – 0.25, interestingly, the shape and intensity of the CD spectrum gradually changed as the mole fraction of dioxane increased. The size of the precipitate was 200 nm as determined by DLS at x = 0.20 as shown in **Fig.2**. CD spectrum of typical α-helix shows double minimum peak around at 208 nm and 222 nm,[21] but the peak around 208 nm was disappeared and only asingle minimum peak at around 225 nm which is characteristic of the β-sheet increased. These changes indicated that an α-helix of myoglobin partially transformed into a β-sheet, and the precipitate became small and solubilized. Dioxane induces hydrogen bonding between peptides, leading to the formation of a secondary structure due to the low relative dielectric constant of dioxane (D = 2.2).[15,22,23] A β-rich transition of myoglobin was also reported under other conditions,[24,25] and this may be a basic metastable structure of myoglobin.

The intensity of the molar ellipticity sharply decreased at x > 0.40 and then fell to zero at x > 0.50. A fine red precipitate was observed in the solution. This is probably because most of the dissolved myoglobin became insoluble due to aggregation. Such a significant decrease in the intensity resulting from protein aggregation was also observed at x = 0.4 in our previous results for cytochrome c with a dioxane system.[15]

As shown in **Fig.1**, the conformation and solubility of myoglobin was strongly dependent on the mole fraction of dioxane. Such a dependence could be related to the properties of the aqueous dioxane solution. Dioxane may weaken the hydrophobic interactions of the protein due to its lower relative dielectric constant compared to water (D = 78.5); the tertiary structure of the protein would therefore be expected to collapse. In our results for other solvents with high dielectric constants, *i.e.*, dimethyl sulfoxide (D = 47) and 1-propanol (D = 20) in aqueous mixtures, the aggregation temperature of cytochrome c was higher than that in aqueous 1,4-dioxane solution, and the aggregated conformation was different (unpublished data). The low dielectric constant of 1,4-dioxane, showing the ability to both induce an α-helix or β-sheet and weaken hydrophobic interaction, is an important factor with respect to the pre-transition state of thermally induced aggregation. In addition, dioxane may influence the properties of water. Dioxane has a low dielectric constant but is soluble in water at all mole fractions. The properties of aqueous dioxane solution are reflected in a negative excess enthalpy[26] and volume[27] at mole fractions of 0.15 and 0.3, respectively, indicating strong interactions between dioxane and water. X-ray diffraction and NMR also show the formation of clusters in the binary solution, which were significantly dependent on the mole fraction.[28] It is conceivable that the interaction between 1,4-dioxane and water influences interactions between water and the protein, which are necessary for the protein to form a native structure, with the conformational transition then occurring at room temperature.

3.2 DSC and SEM of myoglobin with dioxane

Typical DSC curves of myoglobin in aqueous dioxane solutions at various mole fractions of dioxane are shown in **Fig.3**. At x > 0.4, no thermal peaks were observed within the measured temperature range, since aggregation occurred even at room temperature. At x = 0 and 0.05, an endothermic peak reflecting thermal denaturation of myoglobin was observed. The midpoint temperatures of myoglobin for thermal denaturation (T_d) were approximately 81.0 °C (x = 0) and 56.8 °C (x = 0.05). The endothermic peak was reduced during the second consecutive heating, indicating that the transition was partially irreversible. At x = 0.05, the temperature dependence of the ellipticity and the absorbance of myoglobin at 222 nm were measured (data not shown). A decrease in the ellipticity intensity occurred at 50 °C – 60 °C, indicating a loss of secondary structure resulting from thermal denaturation, and a decrease in the absorbance was observed above 60 °C, indicating reduction of the protein concentration by partial aggregation upon heating.

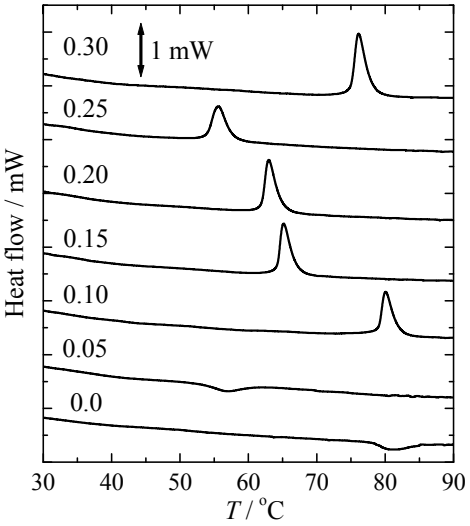

Fig.3 DSC results for myoglobin in (1 − x) water + x dioxane. The numbers in the figure are the mole fractions of dioxane, x. The solution volume and protein concentration are approximately 0.7 ml and 0.5% w/v, respectively, except at x = 0 and 0.05 (0.5 ml and 0.3 % w/v).

Table 1 Transition midpoint temperatures and enthalpy changes of myoglobin for denaturation and aggregation.

x_{Dioxane}	T_d / °C	T_a / °C	ΔH_d / kJ mol^{-1}	ΔH_a / kJ mol^{-1}
0.00	81.0 ± 0.3	-	428 ± 8	-
0.05	56.8 ± 0.5	-	195 ± 15	-
0.10	-	80.1 ± 1.0	-	−565 ± 13
0.15	-	65.2 ± 1.5	-	−610 ± 20
0.20	-	63.0 ± 2.1	-	−633 ± 18
0.25	-	55.6 ± 3.0	-	−549 ± 21
0.30	-	76.1 ± 2.2	-	−809 ± 25

It is noted that no endothermic peak was observed for mole fractions of dioxane >0.10, although this state had a secondary structure at room temperature as revealed by the CD results. The molten globule state, in which the secondary structure exists and the tertiary structure collapses, usually shows endothermic thermal denaturation.[29,30] The absence of an endothermic transition suggests that the state induced by dioxane is an intermediate state, which is thermodynamically close to the thermally denatured state. This phenomenon was also observed for cytochrome *c*.[15] On the other hand, a sharp exothermic peak was observed at $x > 0.10$. No peak was observed for the second consecutive heating, and the red solution of myoglobin became colorless with a red precipitate on heating, indicating that most of the myoglobin irreversibly and exothermically aggregated during the first heating. The obtained midpoint temperatures (T_d and T_a) and the enthalpy changes (ΔH_d and ΔH_a) for thermal denaturation and aggregation, respectively, are listed in **Table 1**. The enthalpy change for the transition was obtained by dividing the measured heat by the total amount of protein in the system.

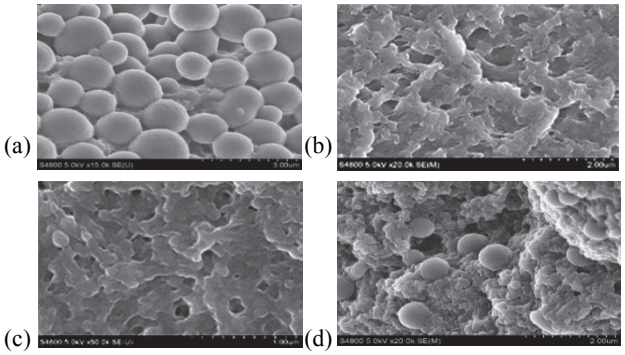

Fig.4 SEM images of thermally induced aggregated myoglobin. (a) dioxane mole fraction, $x = 0.10$; (b) $x = 0.20$; (c) $x = 0.30$; (d) $x = 0.20$ (incubation time = 16.2 h).

Fig.4 shows SEM images of precipitates induced by heating. At $x = 0.10$, where myoglobin forms an α-helix at room temperature, the thermally induced precipitate was a spherical aggregate with a uniform size. On the other hand, at $x = 0.20$, where myoglobin forms a β-sheet at room temperature, the thermally induced precipitate was an amorphous aggregate.
Thus, the structure of the thermally induced precipitate was significantly dependent on the pre-transition structure.

The enthalpy change for the spherical aggregation is −565 kJ mol^{-1} ($x = 0.10$), which is numerically larger than that for the thermal denaturation of the native state, 428 kJ mol^{-1} ($x = 0$), indicating that the aggregate conformation involved many intermolecular interactions. The particle size of the spherical aggregate is 1.0 – 1.5 μm according to SEM, which is larger than that before heating (320 nm from DLS). Since the partial specific volume of monomeric myoglobin in water is approximately 0.747 cm^3 g^{-1}, [20] one particle may be composed of about 3×10^7 protein molecules. Such a large aggregate suggests that many intermolecular associations are formed during a highly exothermic reaction.

On the other hand, the enthalpy change for the amorphous aggregation was −610 to −809 kJ mol^{-1} ($x = 0.15$ to 0.30). T_a and ΔH_a decreased and then increased as the mole fraction of dioxane increased, although the SEM image of the precipitate at $x = 0.3$ was similar to that at $x = 0.2$, as shown in **Fig.4(b)** and **(c)**. **Fig.5** shows plots of ΔH_a at T_a against T_a. Amorphous aggregation from an intermediate state with a β-sheet conformation shows a linear relationship, but spherical aggregation from the α-helical native state does not follow this dependence. The apparent heat capacity change, ΔC_p, associated with the amorphous aggregation obtained from the thermodynamic expression, $\Delta C_p = (\partial \Delta H/\partial T)_p$, was −6.4 kJ mol^{-1} K^{-1}. The negative ΔC_p for the amorphous aggregation suggests that intermolecular association of myoglobin induces a decrease in its accessible surface area, leading to a decrease in hydration. The measured ΔC_p for thermal denaturation of myoglobin was 7.8 kJ mol^{-1} K^{-1}, which is quantitatively similar to that for the amorphous aggregation. This indicates that the increase in the accessible surface area due to thermal denaturation is numerically similar to its decrease due to aggregation.

The ΔH_a for the amorphous aggregation (−809 kJ mol^{-1}, $x = 0.30$) was larger than that for spherical aggregation (−565 kJ mol^{-1}, $x = 0.10$), though T_a was similar (76.1 °C and 80.1 °C). It is suggested that the amorphous aggregation involves more interaction than the spherical aggregation. Given that $\Delta G = 0$ kJ mol^{-1} at T_a, the entropy changes for amorphous and spherical aggregation at T_a were estimated to be −2.32 and −1.60 kJ mol^{-1} K^{-1}, respectively. These negative entropies for the aggregation suggest that the aggregate is highly ordered via intermolecular interactions.

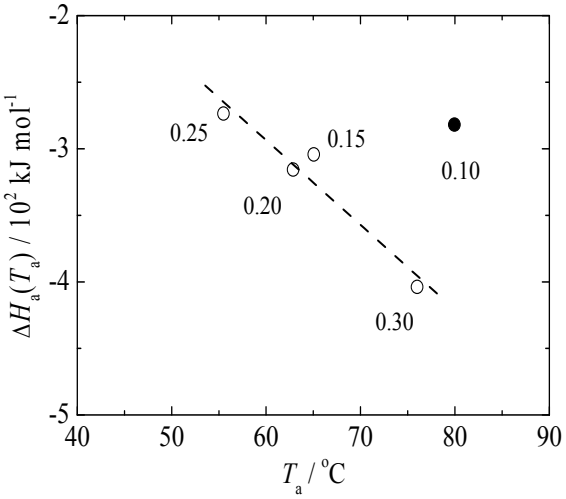

Fig.5 Plot of enthalpy change at T_a against T_a for the aggregation of myoglobin in aqueous 1,4-dioxane solution. The numbers in the figure are the mole fractions of dioxane, *x*. $\Delta H_a(T_a)$ is ΔH_a at T_a. The dashed line was obtained by a linear least squares method, where $r = -0.966$.

Fig.6 shows the state diagram of myoglobin based on the transition temperatures, T_d and T_a. A similar state diagram was observed for cytochrome *c* with a 1,4-dioxane system.[15] At $x = 0 – 0.05$, the helix-rich native state (N) transformed into the thermally denatured state (D_T) upon heating, but not to the ordered spherically aggregated state (SA) within the measured temperature range. At 25°C, the N state transformed into the helix-rich intermediate state (I_α) as the mole fraction increased. The I_α state did not show an endothermic transition upon heating, suggesting that it is thermodynamically close to the D_T state. At $x = 0.125 – 0.30$ and 25°C, the I_α state transformed into the intermediate state with β-sheets (I_β) due to dioxane, and the β-sheet content gradually increased with the mole fraction. At $x > 0.40$ and 25°C, myoglobin aggregated and became insoluble like a dispersed precipitate, as revealed by a significant decrease in the CD intensity. The I_α state transformed into the SA state upon heating, accompanied by a large exothermic peak. The $I_\beta$state transformed to the amorphous aggregated (AA) state upon heating, accompanied by a large exothermic peak. However, thermal aggregation did not occur at a mole fraction of >0.40, because myoglobin had been previously transformed to the AA state. Thus, the helix-rich pre-transition state is essential for the transition to ordered aggregation such as in the SA state.

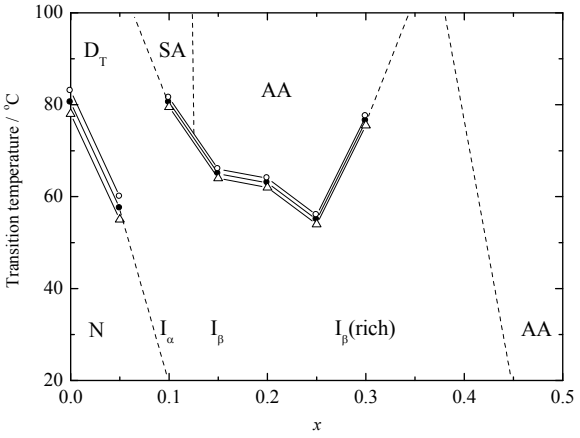

Fig.6 State diagram of myoglobin in (1−x) water + x 1,4-dioxane. The black circles represent T_d and T_a. The triangles and open circles represent 25 % and 75 % of the transition, respectively. N = native state, D_T = thermally denatured state, SA = spherically aggregated state, I_α = helix-rich intermediate state, I_β = beta-sheet-rich intermediate state, and AA = amorphous aggregated state.

3.3 Incubation time dependence

Fig.7 shows the time dependence of the CD spectrum of myoglobin at x = 0.125 and 20°C. The spectrum at 0 h shows single minimum peak at around 225 nm indicating mainly β-sheets. But the intensity and shape of the spectrum gradually changed with time. Relative intensity at 208 nm for 222 nm ($\theta_{208}/\theta_{222}$) was 0.425 at 0 h increased to 0.583 at 6 h indicating that the α-helical content increased because α-helix shows double minimum peak around at 208 nm and 222 nm.[21] The diameter of the protein particles in solution was 320 nm as determined by DLS at 0 h, but large particles with a size of 3 – 4 μm were observed with time. These results indicate that the major reason for the decrease in the CD intensity with time is probably the decrease in protein concentration due to aggregation at 20 °C. The rate constant for the aggregation obtained by assuming a primary reaction was 0.195 h^{-1}, which reflects a slower reaction compared with 3.21 ms^{-1} and 7.79 ms^{-1} for folding and unfolding of myoglobin.[30] This is because the folding and unfolding of monomeric protein is a relatively fast reaction due to rearrangement of the interactions within a protein molecule, but the aggregation is caused by intermolecular interactions between proteins. Such structural change at room temperature would greatly influence the structure of the thermally induced aggregated state because the pre-transition state is important for the thermal transition, as shown in the state diagram.

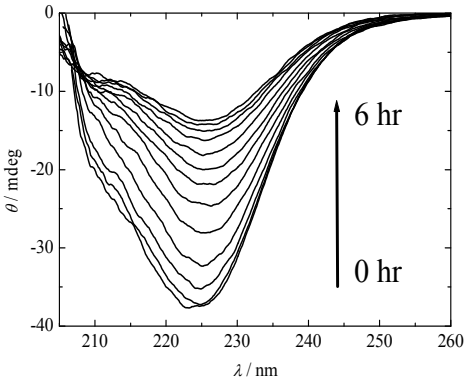

Fig.7 Time dependence of CD spectrum of myoglobin in aqueous 1,4-dioxane solution at x = 0.125 and 20 °C. The protein concentration is about 0.05 %.

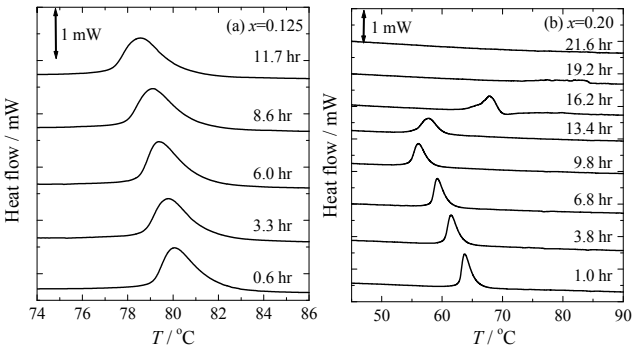

Fig.8 Incubation time dependence of DSC of myoglobin in aqueous 1,4-dioxane solution. (a) x = 0.125; (b) x = 0.20.

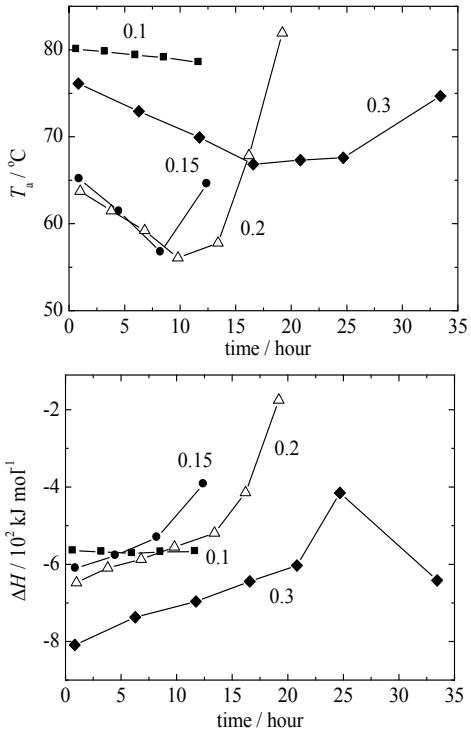

Fig.9 Incubation time dependence of midpoint temperature and enthalpy change for the aggregation of myoglobin in aqueous 1,4-dioxane solution. The numbers in the figure are the mole fractions of dioxane, x.

Fig.8 shows typical DSC results for myoglobin with various incubation times of the pre-transition state at 20°C in aqueous dioxane solution. At x = 0.1, where the pre-transition state is α-helix-rich, the transition temperature slightly shifted to lower temperature with time. On the other hand, at x = 0.2, where the pre-transition state is β-sheet-rich, the transition temperature shifted to lower temperature with time and then returned to higher temperature before disappearing. Such behavior was also observed at x = 0.15 and 0.3 (data not shown), where the pre-transition state is β-sheet-rich. At x = 0.2, the thermally induced aggregated state at an incubation time of 6.8 hours was amorphous as at 0 h. However, the thermally induced aggregated state at an incubation time of 16.2 hours had a partially spherical shape as shown in **Fig.3(d)**, probably because the pre-transition state had some α-helical content. **Fig.9** shows the incubation time dependence of T_a and ΔH_a at each mole fraction. T_a decreases and then increases with time at x > 0.15, where the pre-transition state is β-sheet-rich, although it is almost independent of the incubation time at x = 0.1 where the pre-transition state is α-helix-rich. The ΔH_a numerically

decreases with time except for 34 hours at x = 0.3. These changes are probably due to aggregation in the pre-transition state at room temperature, as reflected by the large particles with a size of 3 – 4 μm and the gradual decrease in CD intensity as shown in **Fig.7**. The T_a increases after a certain time since a spherical aggregate is partially formed by heating due to an increase in the α-helical content. No such significant time dependence was observed for cytochrome *c* in aqueous dioxane solution.[15] Myoglobin has a more flexible structure than cytochrome *c* as revealed by the large adiabatic compressibility of myoglobin (8.98×10^{-5} MPa^{-1}) compared to cytochrome *c* (0.066×10^{-5} MPa^{-1}).[20] We observed a similar time dependence of T_a and ΔH_a for β-lactoglobulin (unpublished data), whose compressibility is 8.45×10^{-5} MPa^{-1}, indicating that large flexible structures may affect the time dependence.

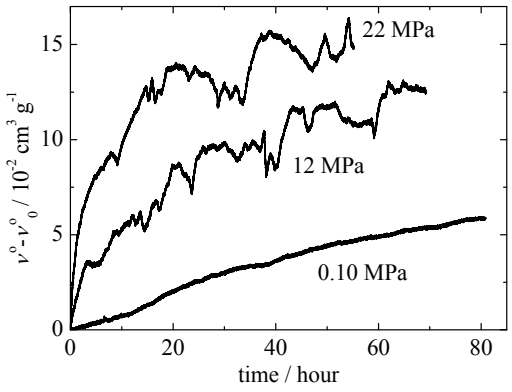

Fig.10 Time dependence of change in apparent partial specific volume of myoglobin at 60°C and x = 0.20 under 0.10, 12, and 22 MPa. The v^o_0 is apparent partial specific volume of myoglobin at 0 hr.

3.4 Activation volume for aggregation

As shown in **Fig.8(b)**, myoglobin is expected to aggregate with time at 60 °C and x = 0.20. **Fig.10** shows the time dependence of the change in partial specific volume of myoglobin under 0.10, 12, and 22 MPa, which gives kinetic and volumetric information for the aggregation. The apparent partial specific volumes increase with time at each pressure. The volume change is approximately 0.04, 0.12, and 0.14 cm^3 g^{-1}, corresponding to 0.72×10^3, 2.16×10^3, and 2.52×10^3 cm^3 mol^{-1}, at 0.1, 12.0, and 22.0 MPa, respectively. Akasaka[31] reported a positive change in partial specific volume (0.041 cm^3 g^{-1}) for the transition to amyloid protofibril at 25°C and atmospheric pressure. The partial specific volume of protein is expressed as the sum of three contributions:[20] (i) the constitutive volume, estimated as the sum of the van der Waals volumes of the constitutive atoms; (ii) the volume of the cavity or void space in the molecule due to imperfect atomic packing; and (iii) the volume change due to hydration or solvation. Such increases in the partial specific volume for the aggregation indicate that intermolecular association forms new cavities between molecules and decreases the degree of hydration by decreasing the accessible surface area of the protein.

The rate constant for the aggregation, k, obtained by assuming a primary reaction, was 0.3×10^{-5}, 1.4×10^{-5}, and 3.9×10^{-5} s^{-1} at 0.1, 12.0, and 22.0 MPa, respectively. The dependence of the rate constant on pressure is related to the activation volume ($V^{\neq}$) according to the thermodynamic relationship,

$$\left(\frac{\partial \ln k}{\partial P}\right)_T = -\frac{V^{\neq}}{RT} \qquad (2)$$

The obtained activation volume of myoglobin for the aggregation is $(-4.5 \pm 1.3) \times 10^2$ cm^3 mol^{-1}, corresponding to a 4 % molar volume of native myoglobin. Seefeldt *et al.* reported a negative activation volume for pressure-induced aggregation of recombinant human interleukin-1 receptor antagonist, $(-1.2 \pm 0.2) \times 10^2$ cm^3 mol^{-1}.[32] This suggests that the activated state for the aggregation has a structure with fewer cavities and/or is highly hydrated compared to the pre-transition state, probably due to partial unfolding.

4. Conclusion

In this study, we determined the thermodynamic and kinetic properties of aggregation of myoglobin by addition of 1,4-dioxane as a co-solvent. The transition enthalpy and entropy for thermally induced aggregation is significantly negative, suggesting that the aggregate contains many interactions and has an ordered structure. The obtained state diagram of myoglobin showed that the SA state can only be formed from the α-helical structure. Depending on the incubation time of the pre-transition state, the thermally aggregated structure changed due to structural changes in the pre-transition state. Since the partial specific volume changes accompanying aggregation were positive, it is considered that the aggregate has a large cavity volume and less hydration. This is consistent with the fact that the apparent heat capacity change for the aggregation is negative. This suggests that the activated state for the aggregation has a structure with fewer cavities and/or is highly hydrated compared to the pre-transition state, probably due to partial unfolding. To better understand the thermodynamic aggregation mechanism, analysis of the influence of the scanning rate and protein concentration is also necessary.

Acknowledgments

The authors gratefully thank the Division of Joint Research Center, Kindai University for the DSC and SEM measurements.

References

1) P. L. Privalov, *Adv. Protein Chem.* **35**, 1–104 (1982).
2) R. L. Baldwin, *Proc. Natl. Acad. Sci. USA* **83**, 8069–8072 (1986).
3) N. Vajpai, L. Nisius, M. Wiktor, and S. Grzesiek, *Proc. Natl. Acad. Sci. USA* **110**, E368–376 (2013).
4) D. J. Selkoe, *Nature* **426**, 900–904 (2003).
5) V. N. Uversky and A. L. Fink Eds., "*Protein Misfolding, Aggregation and Conformational Diseases*", Springer (2006)
6) C. M. Dobson, *Nature* **426**, 884–890 (2003).
7) V. N. Uversky and A. L. Fink, *Biochim. Biophys. Acta* **1698**, 131–153 (2004).
8) L. M. Luheshi, D. C. Crowther, and C. M. Dobson, *Curr. Opin. Chem. Biol*. **12**, 25–31 (2008).
9) S. Parthasarathy, F. Long, Y. Miller, Y. Xiao, D. McElheny, K. Thurber, B. Ma, R. Nussinov, and Y. Ishii, *J. Am. Chem. Soc*. **133**, 3390–3400 (2011).
10) R. Tycko, *Neuron* **86**, 632–645 (2015).
11) M. T. Colvin, R. Silvers, Q. Z. Ni, T. V. Can, I. Sergeyev, M. Rosay, K. J. Donovan, B. Michael, J. Wall, S. Linse, and R. G. Griffin, *J. Am. Chem. Soc*. **138**, 9663–9674 (2016).
12) J. Kardos, K. Yamamoto, K. Hasegawa, H. Naiki, and Y. Goto, *J. Biol. Chem.* **279**, 55308–55314 (2004).
13) K. Sasahara, H. Yagi, H. Naiki, and Y. Goto, *J. Mol. Biol.* **372**, 981–991 (2007).
14) M. So, H. Tagi, K. Sakurai, H. Ogi, H. Naiki, and Y. Goto, *J. Mol. Biol.* **412**, 568–577 (2011).

15) T. Marutani, T. Inomata, and T. Kamiyama, *Thermochim. Acta* in Press, DOI: https://doi.org/10.1016/j.tca.2017.11.003.
16) G. Barone, C. Giancola, and A. Verdoliva, *Thermochim. Acta* **199**, 197–205 (1992).
17) W. Dzwolak, R. Ravindra, J. Lendermann, and R. Winter, *Biochemistry* **42**, 11347–11355 (2003).
18) M. Fändrich, V. Forge, K. Buder, M. Kittler, C. M. Dobson, and S. Diekmann, *Proc. Natl. Acad. Sci. USA* **100**, 15463–15468 (2003).
19) C. Iannuzzi, R. Maritato, G. Irace, and I. Sirangelo, *Int. J. Mol. Sci*. **14**, 14287–14300 (2013).
20) K. Gekko and Y. Hasegawa, *Biochemistry* **25**, 6563–6571 (1986).
21) G. D. Fasman, Ed., "*Circular Dichroism and the Conformational Analysis of Biomolecules*", Springer (1996).
22) V. N. Uversky, N. V. Narizhneva, S. O. Kirschstein, S. Winter, and G. Löber, *Folding and Design* **24**, 163–172 (1997).
23) V. A. Sirotkin, *Biochim. Biophys. Acta* **1750**, 17–29 (2005).
24) C. C. Chow, C. Chow, V. Raghunathan, T. J. Huppert, E. B. Kimball, and S. Cavagnero, *Biochemistry* **42**, 7090–7099 (2003).
25) E. Fabiani, A. M. Stadler, D. Madern, M.M . Koza, M. Tehei, M. Hirai, and G. Zaccai, *Eur. Biophys. J.* **38**, 237–244 (2009).
26) T. Suzuki, M. Fujisawa, S. Takagi, and T. Kimura, *J. Therm. Anal. Cal*. **85**, 545–550 (2006).
27) M. Sakurai, *J. Chem. Eng. Data* **37**, 492–496 (1992).
28) T. Takamuku, A. Yamaguchi, M. Tabata, N. Nishi, K. Yoshida, H. Wakita, and T. Yamaguchi, *J. Mol. Liq*. **83**, 163–177 (1999).
29) T. Kamiyama, Y. Sadahide, Y. Nogusa, and K. Gekko, *Biochim. Biophys. Acta*. **1434**, 44–57 (1999).
30) T. Kamiyama, T. Marutani, D. Kato, T. Hamada, K. Kato, and T. Kimura, *J. Therm. Anal. Calorim*. **123**, 1861–1869 (2016).
31) K. Akasaka, A. R. A. Latif, A. Nakamura, K. Matsuo, H. Tachibana, and K. Gekko, *Biochemistry* **46**, 10444–10450 (2007).
32) M. B. Seefeldt, Y. S. Kim, K. P. Tolley, J. Seely, J. F. Carpenter, and T. W. Randolph, *Protein Sci*. **14**, 2258–2266 (2005).

Tadashi Kamiyama
E-mail: kamiyama@chem.kindai.ac.jp